Published in final edited form as:
Nat Cell Biol. 2014 October ; 16(10): 962–8. doi:10.1038/ncb3035.

RASSF1A-LATS1 signalling stabilises replication forks by restricting CDK2-mediated phosphorylation of BRCA2

Dafni-Eleftheria Pefani[1], **Robert Latusek**[1], **Isabel Pires**[1], **Anna M. Grawenda**[1], **Karen S. Yee**[1], **Garth Hamilton**[1], **Louise van der Weyden**[2], **Fumiko Esashi**[3], **Ester M. Hammond**[1], and **Eric O'Neill**[1,*]

[1]CRUK/MRC Oxford Institute, Dept. of Oncology, University of Oxford, Oxford, OX3 7DQ, UK

[2]The Wellcome Trust Sanger Institute, Hinxton, Cambridge, CB10 1HH, UK

[3]Dunn School of Pathology, South Parks Road, University of Oxford, Oxford, OX1 3RE, UK

Abstract

Genomic instability is a key hallmark of cancer leading to tumour heterogeneity and therapeutic resistance. BRCA2 has a fundamental role in error-free DNA repair but additionally sustains genome integrity by promoting RAD51 nucleofilament formation at stalled replication forks. CDK2 phosphorylates BRCA2 (pS3291-BRCA2) to limit stabilising contacts with polymerised RAD51, however, how replication stress modulates CDK2 activity and whether loss of pS3291-BRCA2 regulation results in genomic instability of tumours is not known. Here we demonstrate that the hippo pathway kinase LATS1 interacts with CDK2 in response to genotoxic stress to constrain pS3291-BRCA2 and support RAD51 nucleofilaments, thereby maintaining genomic fidelity during replication stalling. We also show that LATS1 forms part of an ATR mediated response to replication stress that requires the tumour suppressor RASSF1A. Importantly, perturbation of the ATR-RASSF1A-LATS1 signalling axis leads to genomic defects associated with loss of BRCA2 function and contributes to genomic instability and 'BRCA-ness' in lung cancers.

Replication stress occurs when the progression of a DNA replication fork is impeded by base lesions, insufficient nucleotides (e.g. hydroxyurea, hypoxia) or oncogene enforced errors and is typified by accumulation of single stranded DNA (ssDNA)[1-5]. Increasing evidence suggests that failure to appropriately protect this ssDNA leads to nucleolytic attack, compromising the integrity of nascent DNA at stalled forks and results in increased chromosomal aberrations in human precancerous lesions[6-9]. Recently, components of the Homologous Recombination (HR) pathway have been identified to have a repair independent function that protects nascent DNA at stalled replication forks[8-11]. BRCA1/2

*corresponding author eric.oneill@oncology.ox.ac.uk Tel. 0044 (0) 1865 617321 .

Author contributions DE.P. designed and performed the majority of the experiments, analysed data and contributed to writing the paper; R.L. performed initial experiments for LATS1/CDK2 interaction, γH2AX analysis, pBRCA2 western blots and I-SceI assay; I.P. transferred the DNA fiber technology; G.H. performed the *in vitro* kinase assays; A.G. performed the TCGA analysis; L.v.d.W. isolated Rassf1A$^{-/-}$ mouse embryonic fibroblasts; F.E. provided BRCA2 reagents and advice. E.H. helped with reagents and advice. E.O'N conceived, coordinated and supervised the project, designed experiments, analysed data and wrote the paper.

Europe PMC Funders Author Manuscripts

and FANCD2 tumour suppressors promote the formation of RAD51 nucleofilaments on ssDNA at stalled forks to prevent MRE11 nucleolytic activity and thereby facilitate restart after resolution of replication stress[8-10,12,13]. Failure to efficiently stabilise RAD51 nucleofilaments at stalled forks leads to DNA damage and is purported to be the source of the genomic instability observed in BRCA1/2 mutation carriers and Fanconi Anaemia patients[9].

Formation of a nucleofilament requires initial association of RAD51 monomers with BRC repeats of BRCA2 before polymerisation onto ssDNA. An additional contact of polymerised RAD51 with the C-terminal TR2 domain of BRCA2 stabilises the nucleoprotein filament specifically at replication forks[14,15]. CDK dependent phosphorylation of S3291 within the TR2 domain of BRCA2 decreases binding affinity for polymerised RAD51, resulting in nucleofilament disruption[16]. Upon genotoxic stress, levels of pS3291-BRCA2 are reported to decrease to ensure that RAD51 filament stabilisation can contribute to fork protection and HR[8,16].

LATS1 is a central Ser/Thr kinase of the hippo (MST) tumour suppressor pathway[17,18] that restricts malignant transformation[19]. We previously reported that activation of MST2 in response to DNA damage requires direct phosphorylation of RASSF1A on S131 by the apical sensor of DNA double strand breaks, ATM. In response to ATM activation, MST2 targets LATS1 which in turn phosphorylates the transcriptional co-activator YAP1 promoting its interaction with p73 and induction of apoptosis[20]. Phosphorylation of Ser131 promotes RASSF1A dimerisation and orientates the associated MST2 monomers to allow stimulation of MST2 kinase activity[20]. The minor allele of a common Single Nucleotide Polymorphism (SNP) (*RASSF1* c.397G>T) results in RASSF1A-A133S, which fails to get phosphorylated by ATM or activate MST2/LATS1[21] and is associated with poor overall survival and early cancer onset in BRCA2-mutation carriers[22-24]. RASSF1A is also a frequent site of epigenetic inactivation in sporadic human malignancies with increasing prognostic significance across multiple tumour types[25-27]. Thus, loss of function via genetic or epigenetic routes can lead to RASSF1A inactivation, loss of hippo pathway signalling and promotes malignant transformation.

LATS1 was identified in a screen for ATM/ATR responsive substrates that are required for genomic stability[28]. In this study we show that in response to fork stalling LATS1 interacts with CDK2, restricting pS3291-BRCA2 and thereby facilitating RAD51 nucleofilament stability. This interaction relies on the ATM and Rad3-related kinase (ATR), the main sensor of replication stress[29] that phosphorylates RASSF1A on Ser131 to activate LATS1. We find that the RASSF1A/LATS1 signalling cascade is required during genotoxic stress to support nascent DNA stability at stalled forks. Moreover, we provide evidence that compromised signalling via genetic or epigenetic events leads to accumulation of chromosomal aberrations and introduction of a ‘BRCA-ness’ phenotype in tumours.

Results

LATS1 is necessary for establishment of RAD51 nucelofilaments in response to stress

To gain insight into LATS1 function in response to genotoxic stress we compared the cell cycle profiles of Mouse Embryonic Fibroblasts (MEFs) derived from mice genetically ablated for *Lats1* with their wild type (wt) littermates after exposure in γIR. In line with the findings presented in the genetic screen performed by Matsuoka *et al*[28]., loss of LATS1 through genetic ablation (*Lats1*$^{-/-}$ MEFs) or siRNA mediated silencing, results in enhanced G2/M retention of cells experiencing genotoxic stress (Fig. 1a and Supplementary Fig. 1a). We found that irradiated cells accumulate in G2/M due to elevated levels of γH2AX, a marker of DNA damage and replication fork stalling[12], which persisted in *Lats1*$^{-/-}$ MEFs (Fig. 1b and Supplementary Fig. 1b,d) and LATS1 depleted U2OS cells (Supplementary Fig. 1c,e) but was resolved in control cells. To confirm that high γH2AX levels are indeed due to increased DNA damage, cells were subjected to alkaline single-cell electrophoresis where bright comet tails indicate chromatin unwinding as a result of DNA breaks. As observed for γH2AX, *Lats1*$^{-/-}$ MEFs similarly displayed more DNA breaks (Supplementary Fig. 1f) and re-expression of LATS1 or a kinase dead derivative LATS1-D846A (LATS1-KD) rescued the phenotype, indicating that LATS1 functions to protect against DNA damage independently of kinase activity (Fig. 1b, Supplementary Fig. 1b,d,f). We reasoned that LATS1 either facilitates DNA repair or prevents excessive DNA damage upon genotoxic stress during S phase. Matsuoka *et al.* previously observed that loss of LATS1 leads to increased γH2AX levels and suggested a potential role in HR, the main DNA double strand break repair pathway in S phase cells[28]. To test whether LATS1 facilitates DNA repair via HR, we first assessed recombination competence using the I-SceI assay, where HR activity is required to restore a functional copy of *GFP* and can be scored by FACS. We also monitored RAD51 foci by immunofluorescence as a marker of BRCA2 mediated loading of RAD51 onto resected DNA at break sites which is a prerequisite for HR. Surprisingly, while depletion of LATS1 did not result in significant differences in HR competence (Fig. 1c, Supplementary Fig. 2a), RAD51 foci appeared retarded in response to γIR (Supplementary Fig. 2b). This suggests that elevated γH2AX due to LATS1 ablation is associated with ineffective RAD51 nucleofilament formation. RAD51 catalyses DNA strand exchange to provide a template for HR[30], however, RAD51 also functions in genome protection via a HR independent pathway by forming nucleofilaments that stabilise stalled replication forks[9,10,31].

To determine whether LATS1 contributes to RAD51 foci establishment at stalled forks we depleted nucleotide pools with hydroxyurea (HU) to specifically arrest replication forks. After 6 hours of HU exposure, RAD51 foci were evident in control cells (Fig. 1d) and importantly these were independent of HR associated repair of double strand breaks (p53BP1^{+ve}) that occur at later time points (>10hr HU)[32,33]. In response to HU induced stalled forks, wt MEFs form protective RAD51 filaments on nascent ssDNA, however, RAD51 foci fail to establish in *Lats1*$^{-/-}$ MEFs under the same conditions (RAD51^{+ve}/p53BP1^{-ve} cells in Fig. 1d). Reconstitution of *Lats1*$^{-/-}$ MEFs with either LATS1 or a LATS1 kinase dead derivative (LATS1-KD) restored RAD51 foci, indicating that LATS1 promotes RAD51 nucleofilaments at stalled replication forks (Fig. 1d). We found that MST2

mediated activation of LATS1 is required to establish RAD51 foci, while the classical substrate YAP is dispensable, correlating with a kinase redundant role for LATS1 and a regulatory output for the hippo pathway independent of YAP (Supplementary Fig. 2c). Interestingly, despite the well described role of LATS1 in the regulation of tissue size, discrepancies between the ablation of *Lats1* in mice and conditional expression of constitutive *Yap1* mutants in murine liver suggests the existence of additional mechanisms through which LATS1 suppresses tumour formation[34-36], most notably the potential kinase independent regulation of CDK[37]. Moreover, LATS1 has been shown to interact with CDK1 in mitosis modulating its kinase activity[37].

LATS1 interacts with CDK2 in response to stress and modulates BRCA2 phosphorylation

Exogenous expression of LATS1 homologs bind and restrict CDK kinase activity[37], but the physiological relevance of an endogenous complex has remained elusive. As CDK activity is reported to destabilise RAD51 nucleofilaments, we considered that LATS1 may exert its effects through modulation of CDK activity. In agreement with previous evidence, we were unable to detect an interaction between CDK1/2 and LATS1 in cycling cells, however, upon exposure of cells to γIR or HU induced replication fork stalling, association of endogenous CDK2 and LATS1 was readily observed in reciprocal immunoprecipitates (Fig. 2a). To map the LATS1/CDK2 interaction we generated LATS1 deletion mutants (Fig. 2b) that indicated that binding occurs in the N-terminus (Fig. 2b, lanes 1, 4) and requires residues 1-200 (Fig. 2b, lanes 2, 3 and 5) which encode an Ubiquitin Associated (UBA) domain that directs distinct biological functions of LATS paralogues[38,39]. In line with defective CDK2 association, the LATS1Δ200 derivative was also incapable of establishing RAD51 foci (Fig. 2c). As previously reported for wts/cdc2 and LATS1/CDK1 complexes[37], we find that cyclin partners were excluded from the CDK2 fraction that co-immunoprecipitates with LATS1, leading to loss of substrate targeting and kinase activity (Fig. 2d).

CDK2 mediated C-terminal phosphorylation of BRCA2 leads to unstable RAD51 nucleofilaments[16], therefore we reasoned that LATS1 may facilitate RAD51 foci at stalled forks via preventing phosphorylation of S3291-BRCA2. To test this we addressed pS3291-BRCA2 levels after γIR and HU exposure and found a dramatic elevation of pS3291-BRCA2 in the absence of LATS1, while exogenous LATS1 expression restores control levels (Fig. 2e, Supplementary Fig. 3a). Following γIR, pS3291-BRCA2 levels decrease to facilitate fork stability and HR[16], however loss of LATS1 results in maintenance of phosphorylation levels and correlates with lower RAD51 foci and increased damage (Fig. 1b, d, 2e and Supplementary Fig. 2b). In nocodozol arrested cells, where CDK1 is responsible for pS3291-BRCA2[16,40], higher but identical kinetics to cycling cells were observed, in keeping with LATS1 ability to associate with CDK1 (Supplementary Fig. 3a). Furthermore, *in vitro* phosphorylation of a TR2-domain peptide indicates that CDK2 activity was lower in γIR treated $Lats1^{+/+}$ compared to $Lats1^{-/-}$ MEFs (Supplementary Fig. 3b). Together, these data provide a model where LATS1 binds CDK2, inhibiting BRCA2-TR2 domain phosphorylation and allows RAD51 filament assembly on ssDNA in response to genotoxic stress.

Activation of RASSF1A by ATR is necessary for LATS1 binding to CDK2

In response to DNA damage, RASSF1A activates the hippo cascade via MST2 and LATS1[20,41]. In H1299 lung cancer cells that lack RASSF1A due to promoter methylation[27], LATS1 is unable to associate with CDK2 in response to either HU or γIR (Fig. 3a lanes 4 and 7), but the interaction was restored upon RASSF1A expression (Fig. 3a, lanes 5 and 8). In response to DNA double strand breaks, ATM targets RASSF1A on S131, but fails to activate the genetic variant RASSF1A-A133S at the same recognition site[21]. In contrast to wt RASSF1A, expression of RASSF1A-A133S could not rescue association with CDK2 (Fig. 3a, lanes 6 and 9). We next addressed the levels of pS3291-BRCA2 in response to stress after RASSF1A depletion and the ability of *Rassf1A* genetically null MEFs (*Rassf1A*$^{-/-}$) to form RAD51 filaments on nascent DNA after exposure to HU. In response to either γIR or HU, pS3291-BRCA2 levels decrease but are maintained in the absence of RASSF1A, indicating a greater level of CDK2 activity (Fig. 3c). Moreover *Rassf1A*$^{-/-}$ MEFs are unable to form stable Rad51 nucleofilaments in response to HU (Fig. 3b).

Short HU treatments that do not result in double strand breaks lead to ATR rather than ATM activation, which then elicits appropriate cellular responses to both protect stalled DNA forks and promote resolution of breaks or lesions[29]. ATM recognition sites have been shown to be frequently targeted by ATR in response to single strand breaks or replication stress[42,43], prompting us to consider that RASSF1A may be targeted by ATR in response to fork stalling. To this end, U2OS cells were transiently transfected with FLAG-RASSF1A or FLAG-RASSF1A-A133S and exposed to HU in the presence of a specific ATR inhibitor, VE-821. We found that HU treatment elevates phosphorylation of Ser131 (Fig. 3d, lane 5), while addition of VE-821 inhibits HU dependent increase in pS131-RASSF1A, indicating that RASSF1A is an ATR target (Fig. 3d, lane 8). Similar to ATM mediated targeting, the polymorphic variant did not present any detectable levels of phosphorylation in response to ATR activation (Fig. 3d, lanes 6 and 9). Taken together, the above data highlight that ATR activates the RASSF1A-LATS1-CDK2 cascade in response to replication stress.

Disruption of the RASSF1A/LATS1 axis leads to genomic instability

Failure to establish RAD51 nucleofilaments on ssDNA during replication stalling leads to MRE11 nuclease mediated degradation of nascent DNA and subsequent genomic instability[8-11]. To test whether loss of RASSF1A-LATS1 signalling compromises the stability of nascent DNA at stalled forks we employed DNA fiber analysis to monitor track length of replicated DNA via incorporation of halogenated base analogues that can be detected by immunofluorescence. DNA fibers of *Lats1*$^{+/+}$, *Lats1*$^{-/-}$ and *Lats1*$^{-/-}$ cells expressing mycLATS1 did not differ in the length of CldU (nascent DNA) (Supplementary Fig. 4a). However, after 5 hours of HU treatment CIdU tracks appeared shorter in *Lats1*$^{-/-}$ MEFs in comparison to *Lats1*$^{+/+}$ MEFs (6.6 ± 0.14 and 10.09 ± 0.2 μm respectively, *p=0.0001*) and were restored after re-expression of mycLATS1 (10.3 ± 0.6 μm, *p=0.02*) (Fig. 4a and Supplementary Fig. 4c). To establish whether shorter CIdU tracks in the absence of LATS1 is due to the exposure of the nascent DNA to MRE11 nucleolytic activity, the specific MRE11 inhibitor mirin was used during the HU treatment. *Lats1*$^{-/-}$ MEFs that were treated with mirin, present CIdU tracks with a similar length to control MEFs (8.9 ± 0.91 and 9.2 ± 0.8 μm respectively) (Fig. 4b). RASSF1A ablation had identical effects on fork

integrity (CIdU length in *Rassf1A*$^{+/+}$ vs *Rassf1A*$^{-/-}$ MEFs of 8.8 ± 0.4 and 5.1 ± 0.3 μm respectively, *p=0.01*), which were efficiently rescued by the re-expression of FLAG-RASSF1A (8.08 ± 0.6 μm) but not the polymorphic mutant (5.3 ± 0.1 μm) (Fig. 4c, Supplementary Fig. 4b, d), indicating that ATR phosphorylation of RASSF1A is necessary to protect nascent DNA at stalled forks. Interestingly, both *Lats1*$^{-/-}$ and *Rassf1A*$^{-/-}$ MEFs show shorter second label IdU tracks (Supplementary Fig. 5a, b) indicating defective replication restart after the HU removal, which is independent of MRE11 nucleolytic activity (Fig. 4b). RAD51 has been proposed to facilitate fork regression and formation of a Holliday junction intermediate or "chickenfoot", which offers a more favourable substrate for restart[12,13] and maybe regulated by components that protect fork integrity[44], including RASSF1A and LATS1 .

To determine whether compromised fork integrity in the absence of the RASSF1A/LATS1 axis leads to genomic instability and properties of defective BRCA2 regulation[8], we prepared metaphase spreads from *Lats1*$^{-/-}$ and *Rassf1A*$^{-/-}$ MEFs and checked for typical chromosomal aberrations compared to controls. In line with previous identification of lagging chromosomes in *Rassf1A*$^{-/-}$ mice[45], addition of HU results in increased accumulation of chromosomal aberrations both in the *Lats1* and *Rassf1A* null genetic backgrounds compared to MEFs from littermate controls (aberrations/metaphase: *Lats1*$^{+/+}$ 0.45 vs *Lats1*$^{-/-}$ 4.1 and *Rassf1A*$^{+/+}$ 0.6 vs *Rassf1A*$^{-/-}$ 4.0) indicating that deletion of the RASSF1A/LATS1 axis induces a 'BRCA-ness' phenotype after exposure to stress (Fig. 5a, b and Supplementary Fig. 6a). Similarly, depletion of either LATS1 or RASSF1A from U2OS, increased chromosome aberrations (aberrations/metaphase: control 0.5 vs siLATS1 1.4 or siRASSF1A 1.5, Fig. 5c and Supplementary Fig. 6b) and the number of micronuclei arising from DNA fragments of broken chromosomes (9.6% in siNT versus 18.4% in siLATS1 and 18.2% in siRASSF1A respectively, Supplementary Fig. 6d). Moreover the endemic genomic instability observed in H1299 cells exposed to HU (RASSF1A^{methylated}), was rescued by re-expression of RASSF1A, but not by the polymorphic variant, explaining the predisposition to tumourigenesis of patients that carry this variant (Fig. 5d and Supplementary Fig. 6c)[23]. Moreover, depletion of LATS1 with siRNA ablated the RASSF1A mediated protection of replication stressed H1299 cells, suggesting that RASSF1A contributes to the maintenance of genomic stability via LATS1 (Fig. 5d, Supplementary Fig. 6c).

Methylation of *RASSF1* is a prognostic factor for poor overall survival in lung cancer and decreased therapeutic efficiency to DNA damaging agents in the clinic[46]. To test our hypothesis that this is due to genomic instability, we used publicly available data from the Cancer Genome Atlas (TCGA) that contains genomic characterization data and sequence analysis of tumour genomes. Using the lung adenocarcinoma cohort, which displays frequent hypermethylation of *RASSF1*, we examined possible correlations between *RASSF1A* promoter methylation status and Copy Number Variation (CNV) of the genome. In this cohort (TCGA Lung adenocarcinoma; April 2014), 188 patients had available data and were separated in two groups based on levels of *RASSF1* promoter methylation (low<0.3 and high>0.3) and further divided in 4 subgroups based on the percentage of the genome that was altered (0-0.1%, 0.1-0.2%, 0.2-0.3% and >0.3%). We found an overall correlation between methylation of the *RASSF1* promoter and the extent of genomic

instability (Fig. 6) that is independent of base substitutions (Supplementary Fig. 7); indicative of complex rearrangements that occur after collapsed replication forks observed in Fig. 5. The statistical power is derived from the extremes of the population where relatively stable genomes (<0.1% CNV) have low levels of methylation and unstable genomes (>0.3% CNV) have high methylation of the *RASSF1* promoter (p=0.0054), validating that RASSF1A functions to protect genome integrity (Fig. 6).

Thus, our data describes how ATR promotes BRCA2 dependent replication fork stability and identifies a single nucleotide polymorphism in RASSF1A as an allele displaying 'BRCA-ness'. Moreover, epigenetic loss of RASSF1A in sporadic human malignancies similarly deregulates BRCA2 function, providing a link between the poor prognostic value of RASSF1A loss and BRCA-like phenotypes in common cancers.

Discussion

Previous reports highlighted that depletion of LATS1 leads to genomic instability and tumour predisposition[28,35,37]. We find that LATS1 safeguards genome stability by ensuring stable nucleofilament formation on exposed ssDNA at stalled replication forks (Fig. 7). This is achieved via activation induced conformational changes in LATS1 that stimulate interaction with CDKs as originally suggested by Tao *et al.*[35], and similarly is independent of LATS1 kinase activity. Moreover, in line with identification of LATS1 from screens for regulators of DNA damage[26], the endogenous LATS1-CDK2 interaction occurs in response to replication stress. The core hippo pathway components, RASSF1A and MST1/2 kinase are responsible for activation of LATS1 and are inhibited by growth factor receptor signalling, $KRAS^{WT}$ and RAF1[47-49]. In response to DNA damage, ATM activation results in phosphorylation of RASSF1A on Ser131, activating MST1/2 and LATS1 kinases leading to YAP/p73 proapoptotic complex formation and inhibition of YAP/TEAD mediated malignant transformation[20,41,50]. Failure to activate LATS1 in tumours provides support to $KRAS^{MUT}$ driven oncogenesis through sustained YAP1 transcription[51,52]. However, inefficient activation of LATS1 is likely to have additional effects than solely regulation of YAP1[35-37,39]. In this study we show that MST2 activity is also necessary for the establishment of RAD51 foci at stalled forks but YAP1 is dispensable, providing a new insight into how the core hippo pathway contributes to tumour suppression by maintaining genome integrity.

Schlacher *et al.* proposed that efficient RAD51 nucleofilament formation on nascent DNA of stalled forks is dependent on RAD51 interaction with the TR2 domain of BRCA2 and cannot be restored by re-expression of classical RAD51 binding BRC repeats alone[8,9]. We show that ablation of LATS1 leads to increased pS3291-BRCA2 within the TR2 domain, which prevents RAD51 nucleofilaments during stalling and causes significant shortening in the nascent DNA strands due to MRE11 nucleaolytic activity (Fig. 7). While this is consistent with increased DNA damage, the persistent γH2AX foci after treatment with γIR could also indicate defective DNA repair. Although we did not observe defects in HR, more extensive studies are warranted to determine whether LATS1 plays a role in additional DNA repair pathways. Elevated γH2AX levels may also be attributed to a failure of the fork to restart after resolution of the replication stress. BRCA1/2 and FANCD2 tumour suppressors

were originally described as dispensable for restart[8,9], however, fork recovery is also defective in *Lats1*$^{-/-}$ and *Rassf1A*$^{-/-}$ MEFs which is in line with several studies that indicate a requirementof RAD51 loading for efficient fork restart[12,13]. Moreover FANCD2 was recently reported to interact with BLM and facilitate fork recovery after stress[44]. The proposed role for the nascent DNA and fork regression being required for resolution of stalled fork architecture is controversial but would explain the role for RAD51 in restart.

We show that LATS1-CDK2 interaction and establishment of RAD51 nucleofilaments are RASSF1A dependent. RASSF1A is the most common epigenetically inactivated gene in human tumours. Increasing number of studies have shown that RASSF1A methylation positively correlates with therapeutic resistance and poor survival, indicating the potential utility of RASSF1A as a prognostic/diagnostic marker[25-27,53-55]. The *RASSF1* c.397G>T SNP results in distinct codon usage of Ala instead of Ser at position RASSF1A-133. The minor variant has a sub optimal ATM/ATR activation site and has been reported to act as a dominant allele that correlates with worse prognosis and early cancer onset in BRCA1/2 mutation carriers[21,23,24]. We demonstrate here that ATR activation is necessary for the triggering of the RASSF1A/LATS1 axis and that RASSF1A-Ser133 is unable to stimulate the pathway. Moreover our analysis of lung cancer patients provides a functional insight into how genomic instability and ‘BRCA-ness’ arises in sporadic tumours and may be identified by RASSF1A methylation in a wide variety of tumour types.

Methods

Tissue Culture and Cell treatments

MEFS derived from *Lats1*$^{-/-}$ mice and their WT littermates were obtained from Tian Xu[1]. *Rassf1A*$^{-/-}$ MEFs and their WT littermates were obtained from Louise van der Weyden and David Adams[2]. MEFs were cultured in complete DMEM supplemented with 10% Fatal Bovine Serum in 5% CO_2 and 3% O_2 at 37°C. U2OS, H1299, HT1080 cells were purchased from Cancer Research UK, London or LGC Promochem (ATCC) and cultured in complete DMEM supplemented with 10% Fatal Bovine Serum in 5% CO_2 and 20% O_2 at 37°C. To induce replication stress, cells were treated with 2mM Hydroxyurea (Sigma) for the indicated times. All irradiations were carried out using a Gamma Service® GSRD1 irradiator containing a Cs137 source. The dose rates of the system, as determined by the supplier, were 1.938 Gy/min and 1.233 Gy/min depending on the distance from the source. Cancer cells were transfected with plasmid DNA (2.5 ug/10^6 cells) or siRNA (100nM) using Lipofectamine 2000 (Invitrogen) according to manufacturer’s instructions. MEFs were nucleofected with plasmid DNA or siRNAs using the AMAXA nucleofector (Lonza) according to manufacturer’s instructions. U2OS DR-GFP stable cell line was produced after transient transfection and puromucin selection (1.5ug/ml) of DR-GFP construct (provided by T.Helleday)

DNA constructs and siRNA oligos

The following siRNA oligos were used for targeting in cancer cells: Non Targeting (NT): TAAGGTATGAAGAGATAC; RASSF1A: GACCTCTGTGGCGACTTCA; LATS1:

GGTTCTGAGAGTAAAATTATT; LATS2: CAGGACCTTCACTGGATTAAA; RAD51: CTAATCAGGTGGTAGCTCA

The following siRNA oligos were used for targeting mouse gene expression: LATS2 GeneSolution siRNA (2801009, Qiagen), mouse MST2 (GeneSolution siRNA (2849859, Qiagen), mouse YAP GeneSolution siRNA (2773920, Qiagen).

Myc-LATS1 and Myc-LATS1D846A were kindly provided by H.Sillje[3]. DR-GFP and I-SceI expression plasmids were kindly provided by T.Helleday. FLAG-RASSF1A and FLAG-RASSF1A-133S were previously described[4,5]. LATS1 was PCR cloned into SalI restriction site in the PCMV3b Myc-tagged vector. Δ100LATS1, Δ200LATS1 were PCR-cloned into the PCMV3b Myc-tagged vector between ApaI and SalI sites. ΔC-LATS1 (aa 1-589) and ΔN-LATS1 (aa 589-1130) were PCR-cloned into the PCMV3b Myc-tagged vector at the SalI restriction site.

Antibodies

The following antibodies were used in this study: RAD51 (14B14, GeneTex, GTX702030; 1:500), LATS1 (Bethyl-A300-477; 1:1000), CDK2 (upstate, 07-631; 1:1000), CDK1 (Upstate, 06-923; 1:1000) Cyclin A (BF683, Cell signalling, 4656; 1:1000), Cyclin E (HE12, Cell Signalling, 4129; 1:1000), CyclinB1 (V152, Cell Signalling, 4135; 1:1000), Chk1 (G4, Santa Cruz, sc08408), p-Chk1 (Ser345) (Cell Signalling, 2341; 1:300), MST2 (Epitomics, 1943-1; 1:1000), LATS2 (Novus Biologicals NB200-199; 1:1000), BRCA2 (2B, Calbiochem, OP95; 1:1000), BRDU (BU1/75, Oxford Biotechnology, OBT0030G; 1:500), BRDU (B44, Becton Dickindon, 347580; 1:500), GAPDH (Cell Signalling, 2118; 1:10.000), P53BP1 (Novuls Biologicals, NB100-304; 1:500), γH2AX (Millipore, 05-636; 1:1000), Myc-Tag (JBW301, Millipore, 05-724; 1:1000), FLAG-Tag (M2, Sigma, F3165; 1:1000), pS3291BRCA2 (kindly provided by F. Esashi; 1:1000), pS131RASSF1A previously described (1:1000)[4].

Immunofluorescence

Cells were grown on coverslips and treated as indicated. Cells were fixed with 4% paraformaldehyde, permabilised with 0.3% Triton-X-100 and blocked with 2% BSA in 1×PBS. Coverslips were incubated with the indicated antibodies in blocking solution overnight at 4°C, washed and stained with secondary anti-rabbit and or anti-mouse IgG conjugated with Alexa-Flour 488 or Alexa-Flour 568 (Molecular Probes) for 1h at room temperature. Coverslips were washed with PBS+0.1% Tween and DNA was stained with DAPI. Cells were analysed using LSM780 (Carl ZeissMicroscopy Ltd) confocal microscope. 200-300 cells were scored /condition.

Immunoprecipitations (IPs) and Western Blotting

For LATS1, CDK2 and myc-tagged LATS1 immunoprecipitation, cells were treated as indicated and washed with ice cold PBS prior to lysis. Cells were lysed in 0.5% NP-40 lysis buffer (150 mM NaCl, 20 mM HEPES, 0.5 mM EDTA, 1 mM Na_3VO_4, complete proteinase inhibitor cocktail (Roche)). Total cell extracts were incubated o/n with 20 ul protein G dynabeads (Invitrogen) and 2ug of LATS1, CDK2 or myc-tag antibodies at 4°C. For Flag-

tag immunoprecipitations RIPA lysis buffer was used (50 mM Tris-HCl, 150 mM NaCl, 2mM EGTA, 5 mM MgCl2, 1% v/v NP40, 1% w/v sodium deoxycholate, 0.1% w/v SDS, 10 mM sodium β-glycerophosphate, 50 mM NaF , 1 mM Na_3VO_4, 5 mM sodium pyrophosphate and proteinase inhibitor cocktail EDTA free (Roche) and total cell extracts were immunoprecipitated with 2ug FLAG antibody/ IP at 4° C for 3 hours. Immunoprecipitates were washed 3 times in lysis buffer. Total cell extracts (corresponding to 10% of the immunoprecipitate) and immunoprecipitates were resolved in 4-12% Bis-Tris Nu-PAGE gels (Invitrogen) and transferred onto PVDF membrane (Millipore) before immunoblotting with the appropriate antibodies overnight at 4°C. Primary antibody detection was achieved with Peroxide-conjugated anti-rabbit or anti-mouse antibodies (Jackson Immunoresearch) and exposure to X-Ray film (Kodak). To quantify the bands obtained with western blot analysis, we used ImageJ software (NIH). All bands were normalised against the loading controls.

SceI-induced double-strand break repair

To examine recombination induced by double-strand breakage, U2OS cells stably expressing DR-GFP were transfected with the I-*Sce*I expression vector or pcDNA3.1 as control. 48 hours post transfection, GFP-positive cells were counted using Becton Dickinson FACScan and analysed with CellQuest software (Becton Dickinson).

Propidium Iodide (PI) staining

Cells were treated, collected and fixed in 70% ethanol. Fixed cells were re-hydrated by washing in 1×PBS and re-suspended in 1×PBS containing 50ug/ml PI (Invitrogen, Carlsbad, CA) and 20 ug/ml RNAse (Sigma). Cell cycle profiles analysed with Fluorescence-activated cell sorting (FACS) (FACS Calibur, Becton-Dickinson).

DNA fiber analysis

MEFs were pulse-labelled with 25 uM CldU for 20 min, washed three times with medium, incubated in 2 mM HU for 4 hours, washed three times with medium, and pulse-labelled with 250 uM IdU for 20 min. Labelled cells were harvested, lysed in spreading buffer (200 mM Tris-HCL ph 7.4, 50 mM EDTA, 0.5% SDS) and DNA fibers were spread on slides. CldU and IdU were detected by incubating acid-treated fiber spreads with rat anti-BrdU monoclonal antibody (AbD Serotec) and mouse anti-BrdU monoclonal antibody (Becton Dickinson) for 1 hr at 37°C respectively. Slides were fixed with 4% PFA and incubated with AlexaFluor 555–conjugated goat anti–rat IgG (Molecular Probes) and AlexaFluor 488–conjugated goat anti–mouse IgG (Molecular Probes) for 1 hr at 37°C. Fibers were imaged using an LSM780 (Carl ZeissMicroscopy Ltd) confocal microscope and analysed using ImageJ software (NIH). At least 100 tracks were scored per condition.

Kinase Assay

The CDK2 kinase assay was performed as previously described[6]. Briefly, CDK2 was immunoprecipitated as described above form *Lats1*$^{+/+}$ and *Lats1*$^{-/-}$ MEFs. CDK2 immunoprecipitates were incubated with 2 ug of GST-TR2 peptide substrate in kinase buffer (10mMHepes-HCl pH 7.6, 50 mM β-glycerophosphate, 50 mM NaCl, 10 mM $MgCl_2$, 10

mM $MnCl_2$, 5 μM ATP, 1 mM dithiothreitol, 1 μCi [γ-^{32}P]ATP) for 30 min at 30°C. After 30 min reactions were stopped by the addition of SDS sample buffer and analysed by SDS-PAGE.

Metaphase spreads

U2OS and H1299 cells were transfected with the indicated siRNAs or DNA constructs and 48h post transfection were treated with 2mM HU for 4 hours. After HU removal cells were incubated with 0.1 ug/ml colcemid for 4 hours. MEFs were treated with 2mM HU for 4 hours and after HU removal with 0.2 ug/ml colcemid overnight. Mitotic cells were collected by mitotic shake-off, swollen in hypotonic buffer (10 mM Tris-HCl, pH 7.5, 10 mM NaCl, 5 mM $MgCl_2$) at 37°C for 5 min and spread onto slides. Chromosomes were stained with DAPI.

Alkaline Comet assay

Comet assays were performed as previously described[7]. Cells were trypsinized and embedded in 1% low-melting agarose and lysed in lysis buffer (2.5 M NaCl, 100 mM EDTA, 10 mM Tris base, pH 10.5) for 1h. Slides were washed, followed by incubation in cold electrophoresis buffer (300 mM NaOH, 1 mM EDTA and 1% DMSO, pH > 13) for 30 minutes. Electrophoresis was carried out at 25 V, 300 mA for 25 minutes. Slides were stained with SYBR gold (Invitrogen) after neutralization with 0.5 M Tris-HCl (pH 8.0). Comets were analysed using Komet 5.5 image analysis software (Andor Technology). 50 cells were counted per slide.

TCGA data analysis

The association of the copy number variation (CNV) frequency and mutation count with the *RASSF1* methylation was studied in 554 lung adenocarcinoma patients from the TCGA database for whom complete information on CNV(230), mutation count (231) and *RASSF1* methylation(437) was available. 188 cases had both CNV and methylation information. 115 cases had both mutation count and methylation information.The data was downloaded from cBioPortal for Cancer Genomics [8,9] (Board Institute TCGA Genome Data Analysis Centre (2014): Analysis Overview for Lung Adenocarcinoma (Primary solid tumor cohort) -16 April 2014. Broad Institute of MIT and Harvard Harvard. doi:10.7908/C1TB15K1) and Fisher's exact test was used to compare the differences in frequency distributions.

Statistical Analysis

A two-tailed Student's t test was used for the statistical analysis of immunofluorescence experiments including cells, DNA fibers and metaphase spreads. All experiments were done in triplicates and error bars represent standard deviation (S.D). P values of < 0.05(*), <0.01(**) and <0.001 (***) were considered significant. For clinical samples correlation coefficient was determined with Fisher's exact test. All experiments presented with images (Western Blot analysis) were done in triplicates and representative experiments are shown.

Supplementary Material

Refer to Web version on PubMed Central for supplementary material.

Acknowledgments

The authors would like to acknowledge Thomas Helleday for helpful discussions, Michael Woodcock for FACS analysis and Aswin George Abraham for useful comments on the manuscript. Lats1$^{-/-}$ MEFs were provided by T. Xu and myc-LATS1 constructs by H.Silje. This work was funded by Cancer Research UK A19277, Vertex and the Medical Research Council (MRC). This work was funded by Cancer Research UK A19277, Vertex and the Medical Research Council (MRC).

REFERENCES

1. Olcina MM, et al. Replication stress and chromatin context link ATM activation to a role in DNA replication. Molecular cell. 2013; 52:758–766. doi:10.1016/j.molcel.2013.10.019. [PubMed: 24268576]
2. Petermann E, Helleday T. Pathways of mammalian replication fork restart. Nature reviews. Molecular cell biology. 2010; 11:683–687. doi:10.1038/nrm2974. [PubMed: 20842177]
3. Negrini S, Gorgoulis VG, Halazonetis TD. Genomic instability--an evolving hallmark of cancer. Nature reviews. Molecular cell biology. 2010; 11:220–228. doi:10.1038/nrm2858. [PubMed: 20177397]
4. Murga M, et al. Exploiting oncogene-induced replicative stress for the selective killing of Myc-driven tumors. Nature structural & molecular biology. 2011; 18:1331–1335. doi:10.1038/nsmb.2189.
5. Bartek J, Lukas J. DNA damage checkpoints: from initiation to recovery or adaptation. Current opinion in cell biology. 2007; 19:238–245. doi:10.1016/j.ceb.2007.02.009. [PubMed: 17303408]
6. Halazonetis TD, Gorgoulis VG, Bartek J. An oncogene-induced DNA damage model for cancer development. Science. 2008; 319:1352–1355. doi:10.1126/science.1140735. [PubMed: 18323444]
7. Helmrich A, Ballarino M, Nudler E, Tora L. Transcription-replication encounters, consequences and genomic instability. Nature structural & molecular biology. 2013; 20:412–418. doi:10.1038/nsmb.2543.
8. Schlacher K, et al. Double-strand break repair-independent role for BRCA2 in blocking stalled replication fork degradation by MRE11. Cell. 2011; 145:529–542. doi:10.1016/j.cell.2011.03.041. [PubMed: 21565612]
9. Schlacher K, Wu H, Jasin M. A distinct replication fork protection pathway connects Fanconi anemia tumor suppressors to RAD51-BRCA1/2. Cancer cell. 2012; 22:106–116. doi:10.1016/j.ccr.2012.05.015. [PubMed: 22789542]
10. Hashimoto Y, Ray Chaudhuri A, Lopes M, Costanzo V. Rad51 protects nascent DNA from Mre11-dependent degradation and promotes continuous DNA synthesis. Nature structural & molecular biology. 2010; 17:1305–1311. doi:10.1038/nsmb.1927.
11. Ying S, Hamdy FC, Helleday T. Mre11-dependent degradation of stalled DNA replication forks is prevented by BRCA2 and PARP1. Cancer research. 2012; 72:2814–2821. doi:10.1158/0008-5472.CAN-11-3417. [PubMed: 22447567]
12. Petermann E, Orta ML, Issaeva N, Schultz N, Helleday T. Hydroxyurea-stalled replication forks become progressively inactivated and require two different RAD51-mediated pathways for restart and repair. Molecular cell. 2010; 37:492–502. doi:10.1016/j.molcel.2010.01.021. [PubMed: 20188668]
13. Hashimoto Y, Puddu F, Costanzo V. RAD51- and MRE11-dependent reassembly of uncoupled CMG helicase complex at collapsed replication forks. Nature structural & molecular biology. 2012; 19:17–24. doi:10.1038/nsmb.2177.
14. Esashi F, Galkin VE, Yu X, Egelman EH, West SC. Stabilization of RAD51 nucleoprotein filaments by the C-terminal region of BRCA2. Nature structural & molecular biology. 2007; 14:468–474. doi:10.1038/nsmb1245.
15. Davies OR, Pellegrini L. Interaction with the BRCA2 C terminus protects RAD51-DNA filaments from disassembly by BRC repeats. Nature structural & molecular biology. 2007; 14:475–483. doi:10.1038/nsmb1251.

16. Esashi F, et al. CDK-dependent phosphorylation of BRCA2 as a regulatory mechanism for recombinational repair. Nature. 2005; 434:598–604. doi:10.1038/nature03404. [PubMed: 15800615]
17. Pan D. The hippo signaling pathway in development and cancer. Developmental cell. 2010; 19:491–505. doi:10.1016/j.devcel.2010.09.011. [PubMed: 20951342]
18. Zeng Q, Hong W. The emerging role of the hippo pathway in cell contact inhibition, organ size control, and cancer development in mammals. Cancer cell. 2008; 13:188–192. doi:10.1016/j.ccr.2008.02.011. [PubMed: 18328423]
19. Visser S, Yang X. LATS tumor suppressor: a new governor of cellular homeostasis. Cell Cycle. 2010; 9:3892–3903. [PubMed: 20935475]
20. Hamilton G, Yee KS, Scrace S, O'Neill E. ATM regulates a RASSF1A-dependent DNA damage response. Current biology : CB. 2009; 19:2020–2025. doi:10.1016/j.cub.2009.10.040. [PubMed: 19962312]
21. Yee KS, et al. A RASSF1A polymorphism restricts p53/p73 activation and associates with poor survival and accelerated age of onset of soft tissue sarcoma. Cancer research. 2012; 72:2206–2217. doi:10.1158/0008-5472.CAN-11-2906. [PubMed: 22389451]
22. Kanzaki H, et al. Single nucleotide polymorphism at codon 133 of the RASSF1 gene is preferentially associated with human lung adenocarcinoma risk. Cancer letters. 2006; 238:128–134. doi:10.1016/j.canlet.2005.07.006. [PubMed: 16125301]
23. Gao B, et al. RASSF1A polymorphism A133S is associated with early onset breast cancer in BRCA1/2 mutation carriers. Cancer research. 2008; 68:22–25. doi:10.1158/0008-5472.CAN-07-5183. [PubMed: 18172292]
24. Bergqvist J, et al. RASSF1A polymorphism in familial breast cancer. Familial cancer. 2010; 9:263–265. doi:10.1007/s10689-010-9335-8. [PubMed: 20361264]
25. Wang J, Wang B, Chen X, Bi J. The prognostic value of RASSF1A promoter hypermethylation in non-small cell lung carcinoma: a systematic review and meta-analysis. Carcinogenesis. 2011; 32:411–416. doi:10.1093/carcin/bgq266. [PubMed: 21156971]
26. Jiang Y, Cui L, Chen WD, Shen SH, Ding LD. The prognostic role of RASSF1A promoter methylation in breast cancer: a meta-analysis of published data. PloS one. 2012; 7:e36780. doi:10.1371/journal.pone.0036780. [PubMed: 22615811]
27. Burbee DG, et al. Epigenetic inactivation of RASSF1A in lung and breast cancers and malignant phenotype suppression. Journal of the National Cancer Institute. 2001; 93:691–699. [PubMed: 11333291]
28. Matsuoka S, et al. ATM and ATR substrate analysis reveals extensive protein networks responsive to DNA damage. Science. 2007; 316:1160–1166. doi:10.1126/science.1140321. [PubMed: 17525332]
29. Cimprich KA, Cortez D. ATR: an essential regulator of genome integrity. Nature reviews. Molecular cell biology. 2008; 9:616–627. doi:10.1038/nrm2450. [PubMed: 18594563]
30. Vispe S, Cazaux C, Lesca C, Defais M. Overexpression of Rad51 protein stimulates homologous recombination and increases resistance of mammalian cells to ionizing radiation. Nucleic acids research. 1998; 26:2859–2864. [PubMed: 9611228]
31. Siaud N, et al. Plasticity of BRCA2 function in homologous recombination: genetic interactions of the PALB2 and DNA binding domains. PLoS genetics. 2011; 7:e1002409. doi:10.1371/journal.pgen.1002409. [PubMed: 22194698]
32. Feng Z, Zhang J. A dual role of BRCA1 in two distinct homologous recombination mediated repair in response to replication arrest. Nucleic acids research. 2012; 40:726–738. doi:10.1093/nar/gkr748. [PubMed: 21954437]
33. Hanada K, et al. The structure-specific endonuclease Mus81 contributes to replication restart by generating double-strand DNA breaks. Nature structural & molecular biology. 2007; 14:1096–1104. doi:10.1038/nsmb1313.
34. Dong J, et al. Elucidation of a universal size-control mechanism in Drosophila and mammals. Cell. 2007; 130:1120–1133. doi:10.1016/j.cell.2007.07.019. [PubMed: 17889654]
35. St John MA, et al. Mice deficient of Lats1 develop soft-tissue sarcomas, ovarian tumours and pituitary dysfunction. Nature genetics. 1999; 21:182–186. doi:10.1038/5965. [PubMed: 9988269]

36. Camargo FD, et al. YAP1 increases organ size and expands undifferentiated progenitor cells. Current biology : CB. 2007; 17:2054–2060. doi:10.1016/j.cub.2007.10.039. [PubMed: 17980593]
37. Tao W, et al. Human homologue of the Drosophila melanogaster lats tumour suppressor modulates CDC2 activity. Nature genetics. 1999; 21:177–181. doi:10.1038/5960. [PubMed: 9988268]
38. Li Y, et al. Lats2, a putative tumor suppressor, inhibits G1/S transition. Oncogene. 2003; 22:4398–4405. doi:10.1038/sj.onc.1206603. [PubMed: 12853976]
39. Yabuta N, et al. N-terminal truncation of Lats1 causes abnormal cell growth control and chromosomal instability. Journal of cell science. 2013; 126:508–520. doi:10.1242/jcs.113431. [PubMed: 23230145]
40. Ayoub N, et al. The carboxyl terminus of Brca2 links the disassembly of Rad51 complexes to mitotic entry. Current biology : CB. 2009; 19:1075–1085. doi:10.1016/j.cub.2009.05.057. [PubMed: 19540122]
41. Matallanas D, et al. RASSF1A elicits apoptosis through an MST2 pathway directing proapoptotic transcription by the p73 tumor suppressor protein. Molecular cell. 2007; 27:962–975. doi:10.1016/j.molcel.2007.08.008. [PubMed: 17889669]
42. Traven A, Heierhorst J. SQ/TQ cluster domains: concentrated ATM/ATR kinase phosphorylation site regions in DNA-damage-response proteins. BioEssays : news and reviews in molecular, cellular and developmental biology. 2005; 27:397–407. doi:10.1002/bies.20204.
43. Lopez-Contreras AJ, Fernandez-Capetillo O. The ATR barrier to replication-born DNA damage. DNA repair. 2010; 9:1249–1255. doi:10.1016/j.dnarep.2010.09.012. [PubMed: 21036674]
44. Chaudhury I, Sareen A, Raghunandan M, Sobeck A. FANCD2 regulates BLM complex functions independently of FANCI to promote replication fork recovery. Nucleic acids research. 2013; 41:6444–6459. doi:10.1093/nar/gkt348. [PubMed: 23658231]
45. Song MS, et al. The tumour suppressor RASSF1A regulates mitosis by inhibiting the APCCdc20 complex. Nature cell biology. 2004; 6:129–137. doi:10.1038/ncb1091. [PubMed: 14743218]
46. Endoh H, et al. RASSF1A gene inactivation in non-small cell lung cancer and its clinical implication. International journal of cancer. Journal international du cancer. 2003; 106:45–51. doi:10.1002/ijc.11184. [PubMed: 12794755]
47. Matallanas D, et al. Mutant K-Ras activation of the proapoptotic MST2 pathway is antagonized by wild-type K-Ras. Molecular cell. 2011; 44:893–906. doi:10.1016/j.molcel.2011.10.016. [PubMed: 22195963]
48. O'Neill E, Rushworth L, Baccarini M, Kolch W. Role of the kinase MST2 in suppression of apoptosis by the proto-oncogene product Raf-1. Science. 2004; 306:2267–2270. doi:10.1126/science.1103233. [PubMed: 15618521]
49. Romano D, et al. Protein interaction switches coordinate Raf-1 and MST2/Hippo signalling. Nature cell biology. 2014; 16:673–684. doi:10.1038/ncb2986. [PubMed: 24929361]
50. van der Weyden L, et al. Loss of RASSF1A synergizes with deregulated RUNX2 signaling in tumorigenesis. Cancer research. 2012; 72:3817–3827. doi:10.1158/0008-5472.CAN-11-3343. [PubMed: 22710434]
51. Kapoor A, et al. Yap1 activation enables bypass of oncogenic kras addiction in pancreatic cancer. Cell. 2014; 158:185–197. doi:10.1016/j.cell.2014.06.003. [PubMed: 24954535]
52. Shao DD, et al. KRAS and YAP1 Converge to Regulate EMT and Tumor Survival. Cell. 2014; 158:171–184. doi:10.1016/j.cell.2014.06.004. [PubMed: 24954536]
53. Wang J, et al. Value of p16INK4a and RASSF1A promoter hypermethylation in prognosis of patients with resectable non-small cell lung cancer. Clinical cancer research : an official journal of the American Association for Cancer Research. 2004; 10:6119–6125. doi:10.1158/1078-0432.CCR-04-0652. [PubMed: 15447998]
54. Tanemura A, et al. CpG island methylator phenotype predicts progression of malignant melanoma. Clinical cancer research : an official journal of the American Association for Cancer Research. 2009; 15:1801–1807. doi:10.1158/1078-0432.CCR-08-1361. [PubMed: 19223509]
55. de Fraipont F, et al. An apoptosis methylation prognostic signature for early lung cancer in the IFCT-0002 trial. Clinical cancer research : an official journal of the American Association for Cancer Research. 2012; 18:2976–2986. doi:10.1158/1078-0432.CCR-11-2797. [PubMed: 22434665]

Europe PMC Funders Author Manuscripts

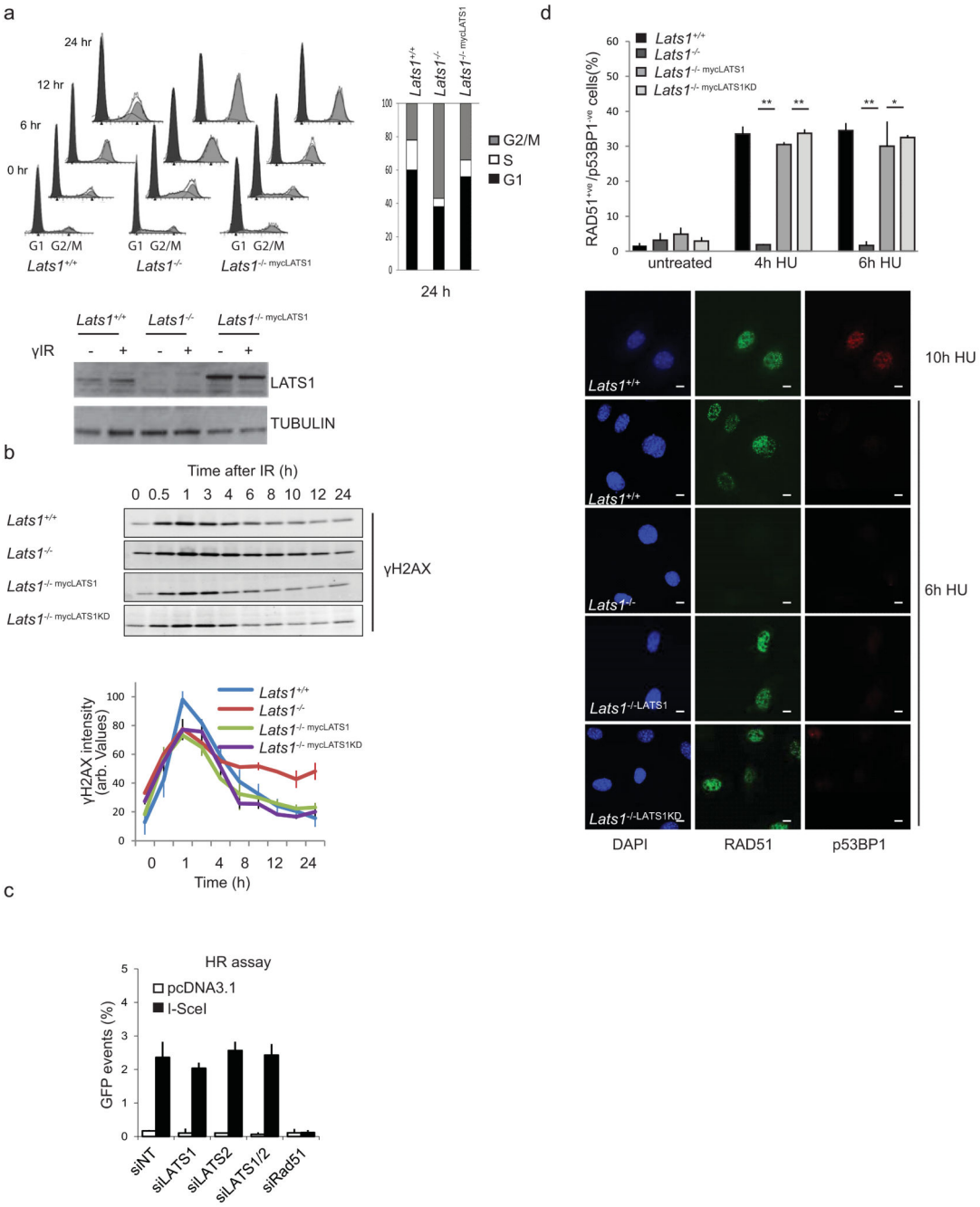

Figure 1. LATS1 regulates RAD51 nucleofilament formation in response to replication stress in an HR independent manner

(a) Propidium Iodide profiles at the indicated time points after exposure to 10 Gy γIR of wild type MEFs, and *Lats1*$^{-/-}$ MEFs transfected with mycLATS1 or control plasmid. The percentage of cells in G1, S and G2/M is shown. **(b)** *Lats1*$^{+/+}$, *Lats1*$^{-/-}$and *Lats1*$^{-/-}$ cells expressing wt hLATS1 (Lats1$^{-/-\text{mycLATS1}}$) or a hLATS1 kinase dead derivative LATS1-D846A (*Lats1*$^{-/-\text{LATS1KD}}$) were treated with 10 Gy γIR. Total cell extracts were isolated at the indicated time points after irradiation and analysed for γH2AX expression. Both wtLATS1 and LATS1KD reconstitute the DNA repair kinetics after damage. Representative

Europe PMC Funders Author Manuscripts

blots are shown. Error bars represent standard deviation from n=3 independent experiments. **(c)** HR assay of a single DNA break induced by I-SceI endonuclease, using the DR-GFP reporter in U2OS cells treated with the indicated siRNAs. GFP-positive cells indicate HR events after I-SceI expression. Error bars represent standard deviation from n=3 independent experiments **(d)** *Lats1*$^{+/+}$, *Lats1*$^{-/-}$, *Lats1*$^{-/-\text{mycLATS1}}$ and *Lats1*$^{-/-\text{mycLATS1KD}}$ MEFs were treated with Hydroxyurea (HU) for 4 or 6 hours, fixed and assessed for RAD51 and p53BP1 foci formation. The percentage of RAD51 positive cells without double strand breaks (negative for p53BP1 staining) was quantified and presented. At least 300 cells were scored per condition in n=3 independent experiments. Error bars represent standard deviation. Statistical significance was determined by a two-tailed t-test. * P< 0.05, ** P<0.01. Scale bar, 10 μm.

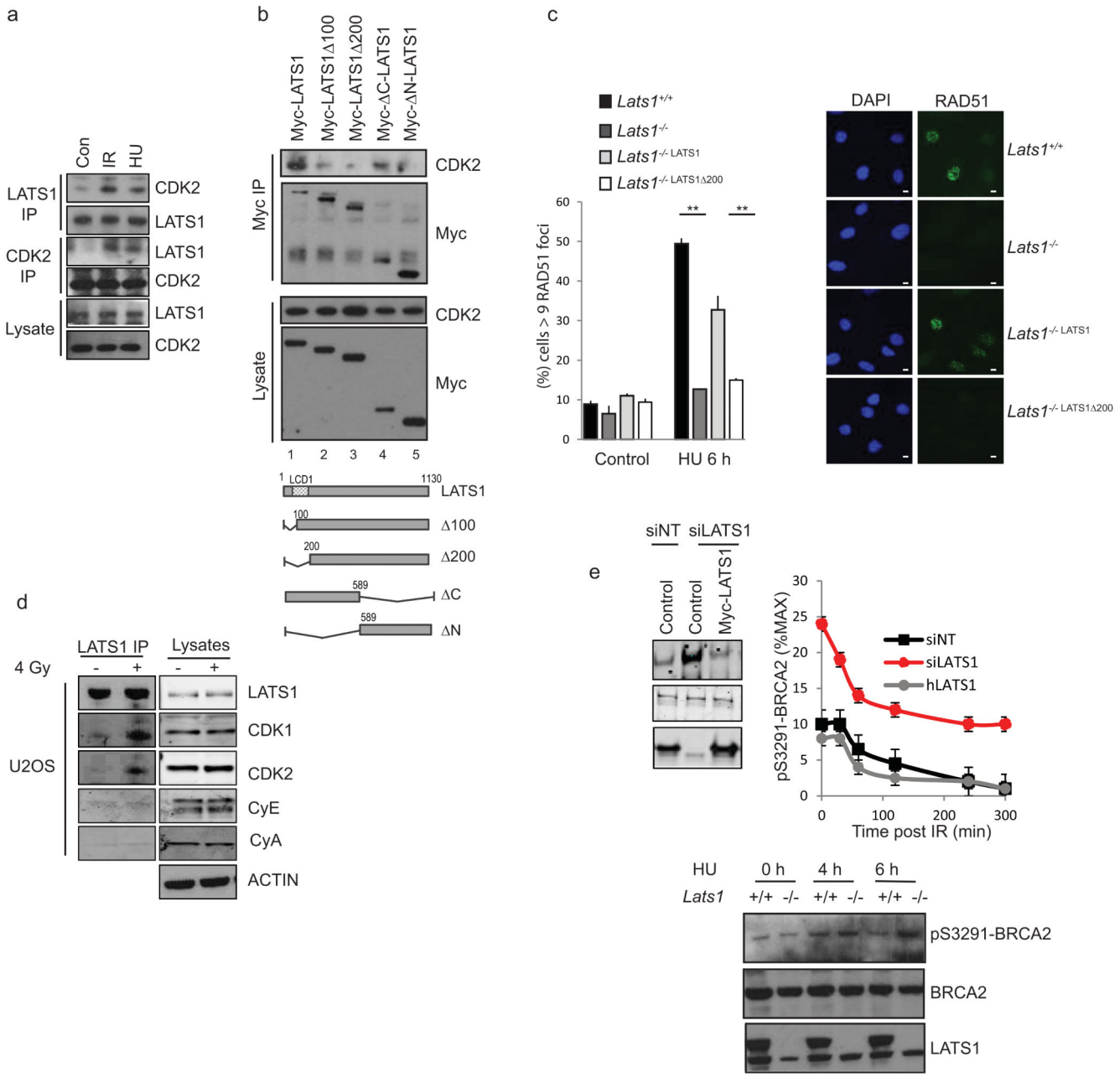

Figure 2. LATS1 interacts with CDK2 in response to genotoxic stress modulating its kinase activity towards BRCA2

(a) U2OS cells were treated with 4 Gy γIR or 2 mM HU for 4 hours, lysed and total cell extracts were immunoprecipitated with LATS1 or CDK2 antibodies. Total cell lysates and immunoprecipitates were analysed by Western Blot and probed with antibodies against LATS1 and CDK2. **(b)** U20S cells were transiently transfected with full length Myc-LATS1 or LATS1 deletion mutants: Myc-LATS1Δ100, Myc-LATS1Δ200, Myc-ΔC-LATS1 (aa 1-589) or Myc-ΔN-LATS1 (aa 589-1130). 48 hours post transfection cells were treated with HU for 4 hours prior to Myc tag immunoprecipitation. Western blot analysis of total cell extracts and immunoprecipitates is shown. **(c)** *Lats1*$^{+/+}$, *Lats1*$^{-/-}$, *Lats1*$^{-/-\text{mycLATS1}}$ and

Europe PMC Funders Author Manuscripts

Europe PMC Funders Author Manuscripts

Lats1$^{-/-mycLATS1\Delta200}$ MEFs were treated with HU for 6 hours, fixed and stained for RAD51. 200 cells were scored per condition in n=3 independent experiments**.** Error bars represent standard deviation. Statistical significance was determined by a two-tailed t-test. ** P<0.01. Scale bar 10 μm. **(d)** Total cell lysates and LATS1 immunoprecipitates of untreated or treated with γIR U2OS cells probed for the indicated antibodies. **(e)** Upper panel, detection of pS3291-BRCA2 in lysates of HT1080 cells transfected with control siRNA or siRNA against LATS1 and pcDNA3.1 (control) or mycLATS1 constructs. 48 hours post transfection cells were subjected to 4 Gy γIR and total cell extracts were collected over a 300 min time course. Line graph represents average densitometry of pS3291-BRCA2 levels as a percentage of max value over the time course presented in Supplementary Fig. 3a and is representative of n=3 independent experiments. Error bars represent % variation in average densitometry from Licor values and ImageJ analysis. Lower panel, *Lats1*$^{+/+}$ and *Lats1*$^{-/-}$ MEFs were treated with HU for the indicated times. Total cell extracts were collected and blotted for pS3291-BRCA2.

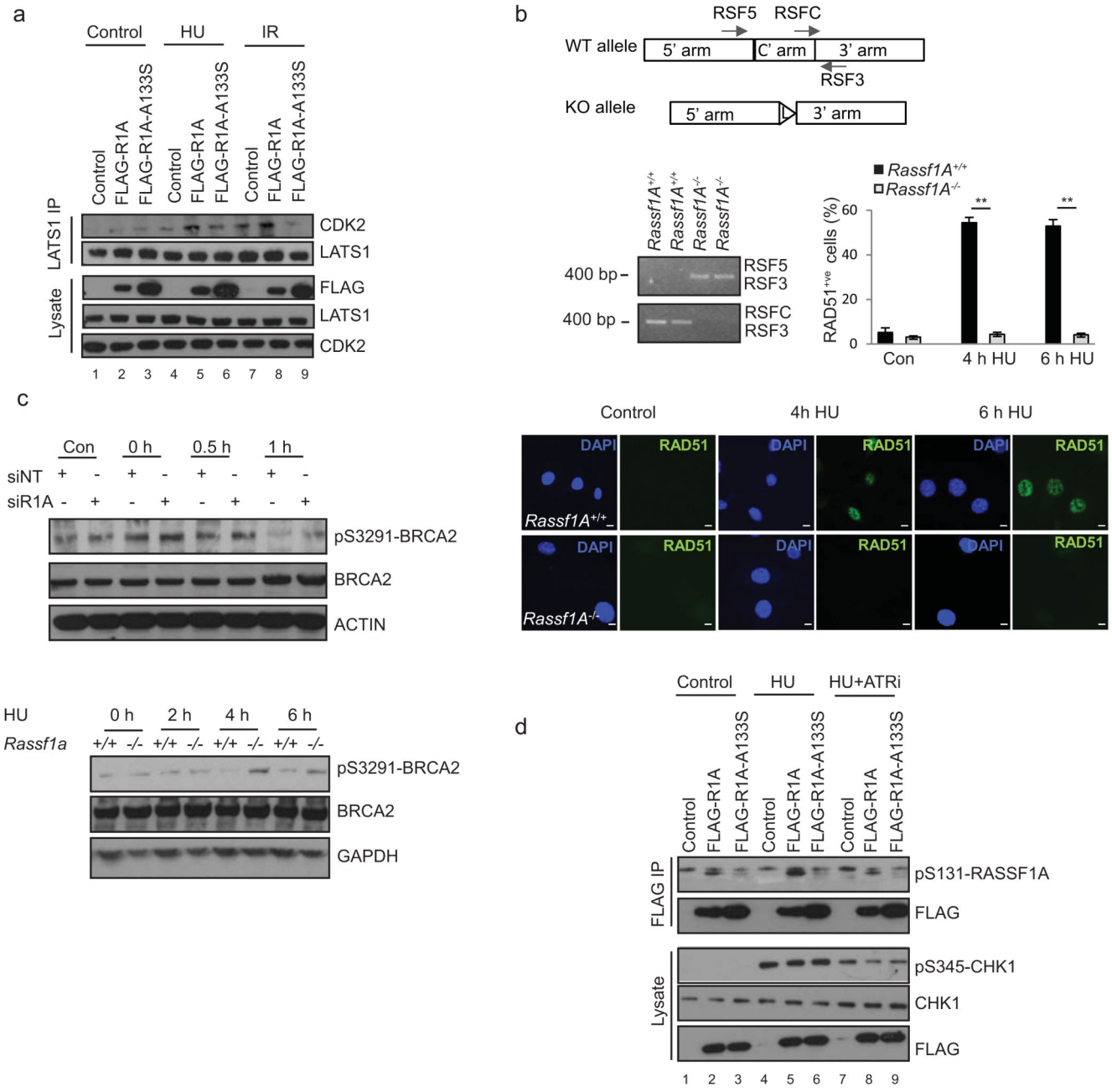

Figure 3. Tumour suppressor RASSF1A stimulates LATS1/CDK2 interaction in response to ATR activation

(a) H1299 cells (methylated *RASSF1 gene* promoter) were transiently transfected with pcDNA3.1, FLAG-RASSF1A (FLAG-R1A) or FLAGR1A-A133S and treated with 2 mM HU for 5 hours or 4 Gy γIR. LATS1 was immunoprecipitated from total cell lysates and co-immunoprecipitation of CDK2 was examined by Western Blot analysis. **(b)** Upper, PCR genotyping of genomic DNA, using a combination of two primer pairs (either RSF-5/RSF-3 or RSF-C/RSF-3), which can distinguish between *Rassf1A*$^{+/+}$ and *Rassf1A*$^{-/-}$ genotypes. Lower, RAD51 foci formation in *Rassf1A*$^{+/+}$ and *Rassf1A*$^{-/-}$ MEFs after exposure to 2 mM

HU for the indicated periods. 200 cells were scored per condition in n=3 independent experiments and bar graph quantified in bar graphs. Error bars represent standard deviation. Statistical significance was determined by a two-tailed t-test, ** P<0.01. Scale bar, 10 μm. **(c)** Upper, U2OS cells were treated with siRNA against RASSF1A or control siRNA (siNT) and subjected to 4 Gy γIR. Cell extracts were collected at the indicated time points and blotted for pS3291-BRCA2. Lower, *Rassf1A*$^{+/+}$ and Rassf1A$^{-/-}$ MEFs were treated with HU for the indicated times. Total cell extracts were collected and blotted for pS3291-BRCA2 **(d)** U2OS cells were transiently transfected with pcDNA3.1, FLAG-R1A or FLAG-R1A-A133S. Cells were treated with 2 mM HU for 5 hours in the presence or absence of the specific ATR inhibitor VE-821. RASSF1A phosphorylation on Ser131 was assessed in FLAG immunoprecipitates.

Europe PMC Funders Author Manuscripts

Europe PMC Funders Author Manuscripts

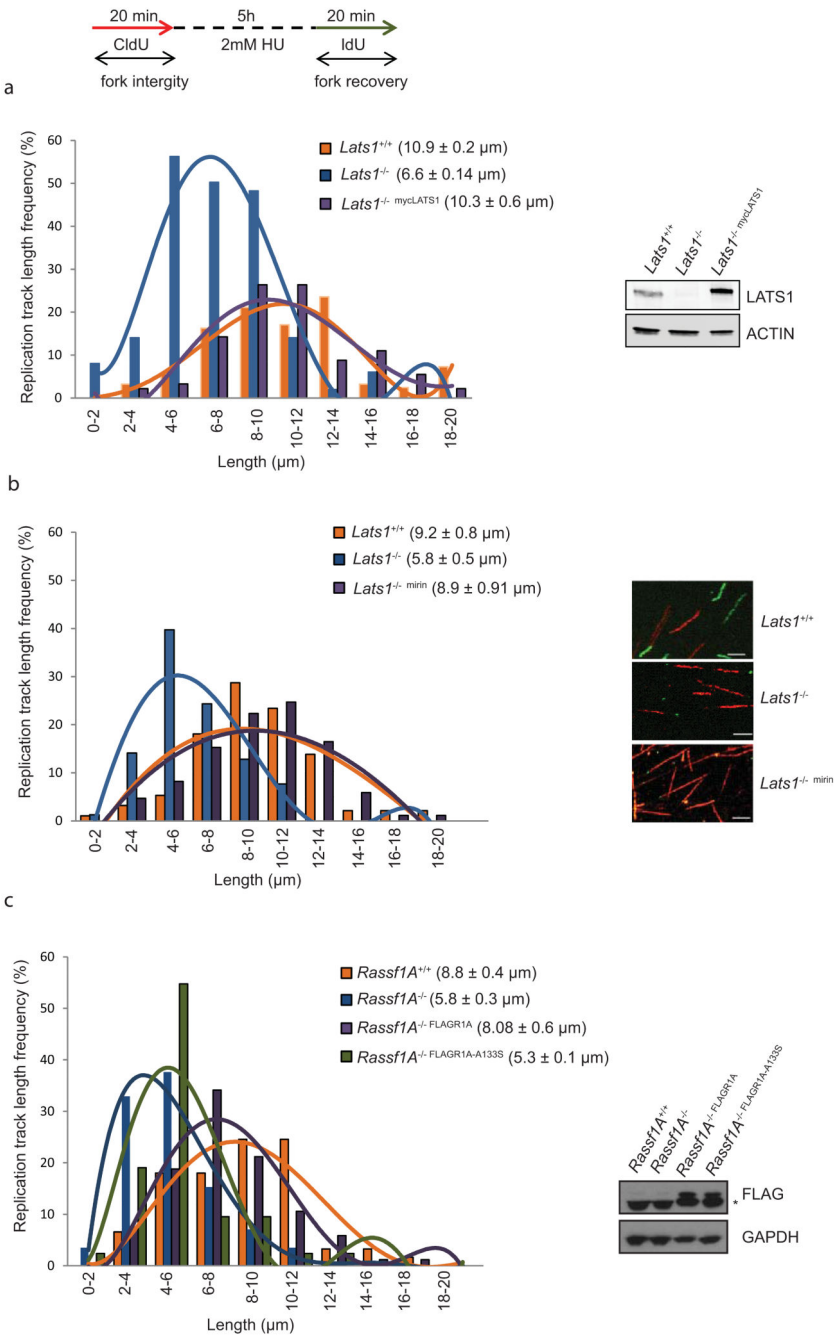

Figure 4. Deletion of RASSF1A/LATS1 axis compromises the stability of nascent DNA at stalled forks

(a) CIdU tract length distributions analysis from DNA fibres from *Lats1*$^{+/+}$, *Lats1*$^{-/-}$and *Lats1*$^{-/-}$mycLATS1 MEFS in the presence of 2 mM HU. Representative pictures for each condition are shown in Supplementary Fig. 4c. Western Blots indicate LATS1 expression. **(b)** CIdU tract length distributions from DNA fibres from *Lats1*$^{+/+}$, *Lats1*$^{-/-}$ and *Lats1*$^{-/-}$ MEFS treated with the MRE11 inhibitor, mirin, after treatment with 2 mM HU and representative pictures for each condition. **(c)** CIdU tract length distributions from DNA

fibres from *Rassf1A*$^{+/+}$, *Rassf1A*$^{-/-}$, *Rassf1A*$^{-/-}$FLAGR1A and *Rassf1A*$^{-/-}$FLAG-R1A-A133 MEFs exposed in 2 mM HU. Representative pictures for each condition are shown in Supplementary Fig. 4d. Western Blots indicate Flag-RASSF1A expression (* indicates non-specific band in MEF lysates). Sketch above delineates experimental design. Bar-graphs derived from representative experiment. Mean track lengths and standard deviation given in parenthesis derived from n=3 independent experiments. Statistical significance was determined by a two-tailed t-test. At least n=100 DNA tracks were scored in each condition. Scale bar, 10 μm.

Europe PMC Funders Author Manuscripts

Europe PMC Funders Author Manuscripts

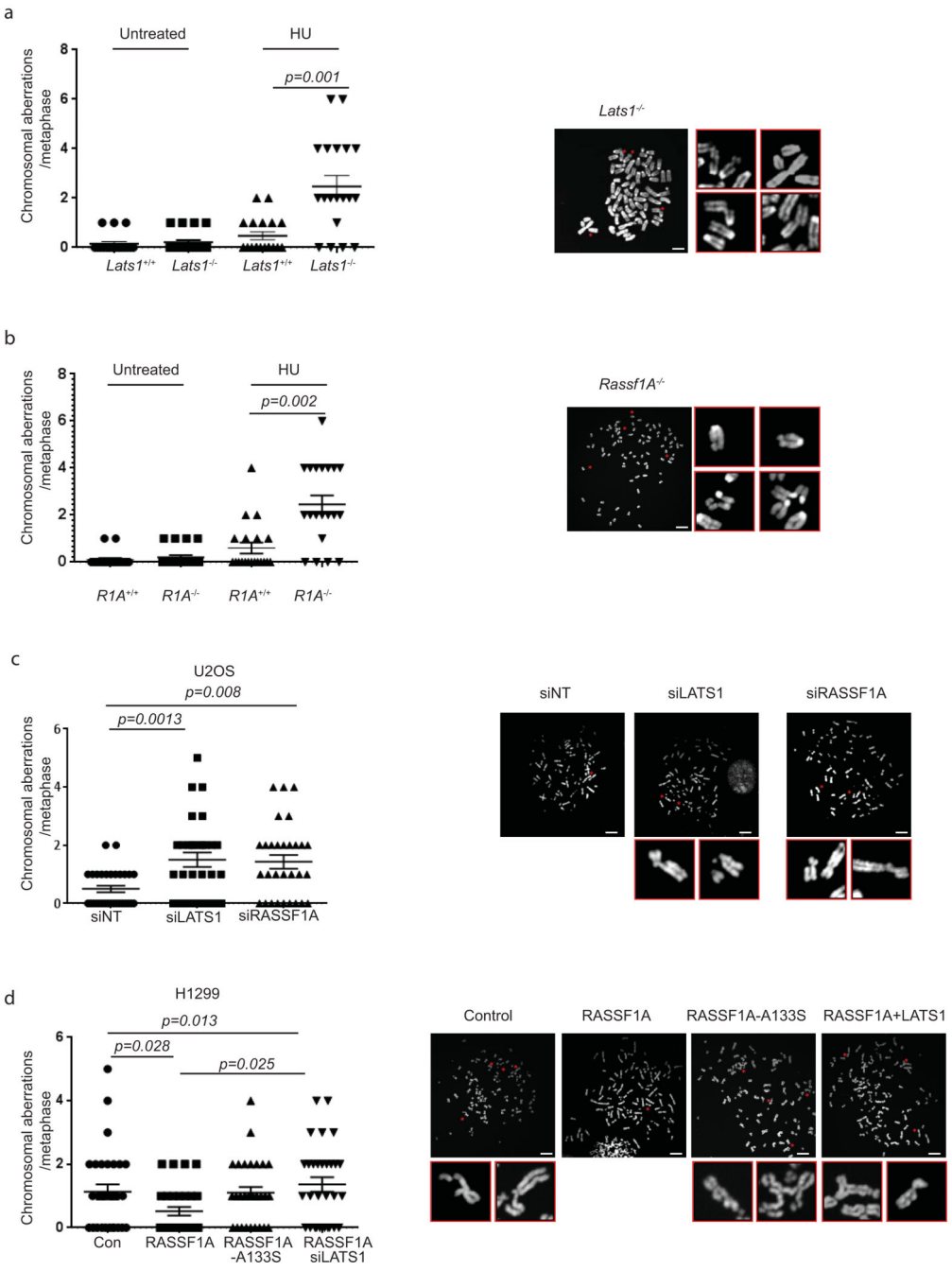

Figure 5. Deletion of RASSF1A/LATS1 axis induces chromosomal aberrations

Number of chromosomal aberrations/metaphase spread of **(a)** *Lats1*$^{+/+}$ and *Lats1*$^{-/-}$ MEFs or **(b)** *Rassf1A*$^{+/+}$ and *Rassf1A*$^{-/-}$ with or without HU prior to colcemid addition. **(c)** U2OS cells were treated with control siRNA or siRNA against LATS1 or RASSF1A and exposed to HU prior to colcemid addition. The number of aberrant chromosomes/metaphase spread and representative metaphase spreads from HU treated cells are displayed. **(d)** H1299 cells were transfected with pcDNA3.1, FLAG-RASSF1A or FLAG-RASSF1A-A133S and exposed to HU prior to colcemid addition. The number of aberrant chromosome/metaphase

in each condition and representative pictures from spreads of HU treated cells are shown. n=20 metaphases from MEFS and n=30 metaphases from cancer cells were scored per condition. Aberrant chromosomes in each metaphase are denoted by red asterisk and displayed in higher magnification. Error bars represent standard error of the mean. Statistical significance was determined by a two-tailed t-test. P values are given on the figure. Scale bar, 10 μm.

Europe PMC Funders Author Manuscripts

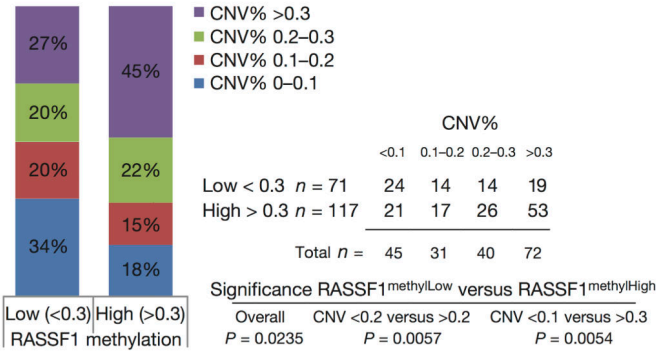

Figure 6. RASSF1A methylation correlates with increased CNV in lung cancer patients

Correlation of RASSF1 promoter methylation (illumina HM450) with genomic Copy Number Variation (CNV) in lung adenocarcinoma dataset from the cancer genome atlas database (TCGA, Provisional). Bar graph representing the percentage of patients in each subgroup based on extent of genome alterations (% of the genome) in cohorts with high (>0.3) or low (<0.3) RASSF1 promoter methylation. A total of 188 patients with Lung Adenocarcinoma were analysed using the Fisher's exact test. Absolute numbers (n) and *p* values are presented in the table.

Europe PMC Funders Author Manuscripts

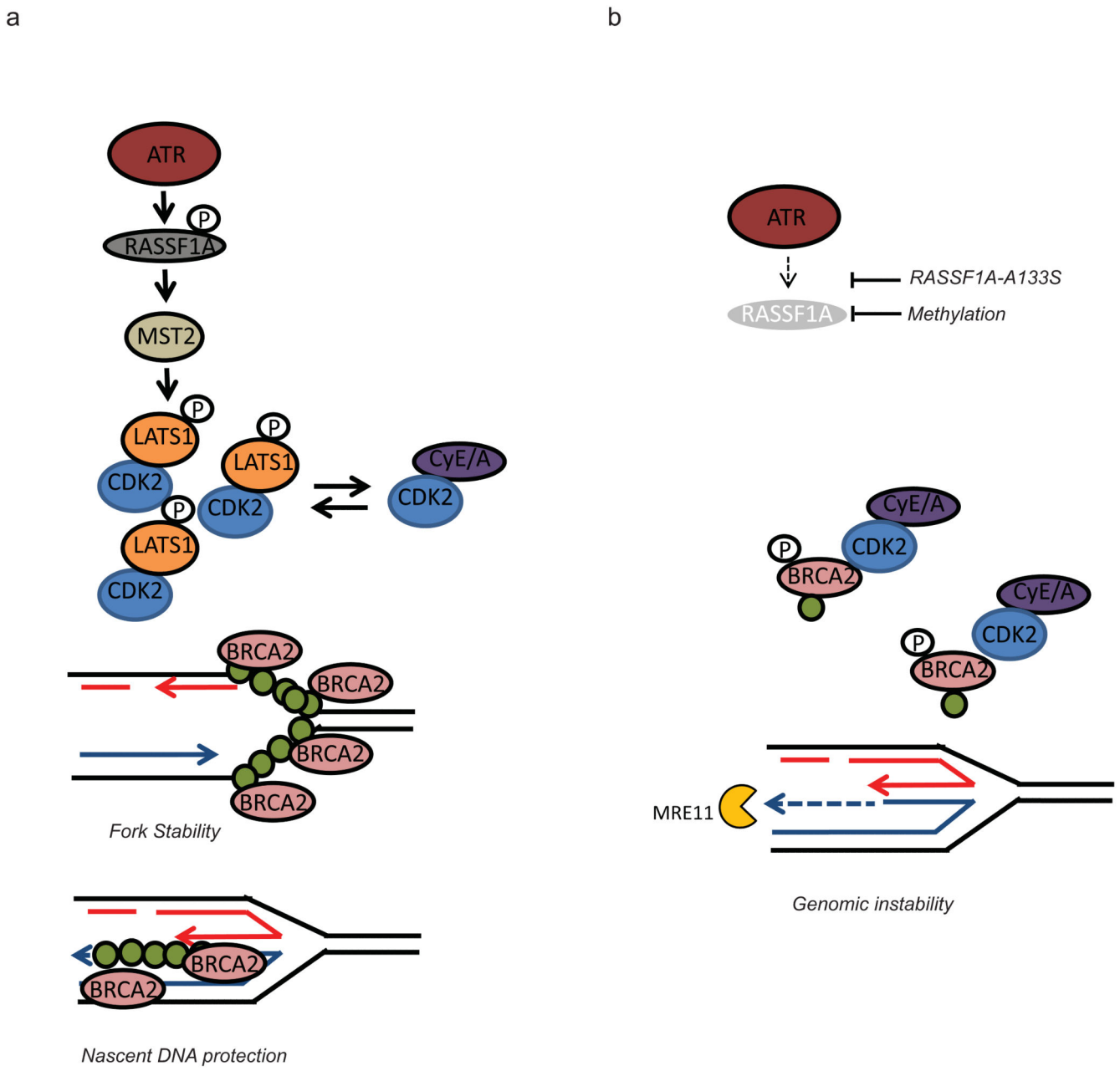

Figure 7. Model of RASSF1A/LATS1/CDK2 signalling and the protection of stalled replication forks

(a) In response to fork stalling and ATR activation, RASSF1A triggers LATS1-CDK2 interaction and restricts CDK2 kinase activity towards BRCA2 promoting the establishment of RAD51 filaments. (b) Upon genetic or epigenetic inactivation of RASSF1A, CDK2 remains active resulting in increased levels of pS3291-BRCA2, exposure of nascent DNA to MRE11 nucleolitic activity and genomic instability.